Nano Today 57 (2024) 102329

Contents lists available at ScienceDirect

Nano Today

journal homepage: www.elsevier.com/locate/nanotoday

Multishaped bio-gold polyphenols bearing nanoparticles to promote inflammatory suppression

Valeria De Matteis [a,b], Mariafrancesca Cascione [a,b], Paolo Pellegrino [a,b], Riccardo Di Corato [b], Massimo Catalano [a,b], Alessandro Miraglia [d], Aurelia Scarano [d], Angelo Santino [d], Marcello Chieppa [c], Rosaria Rinaldi [a,b,*]

[a] Department of Mathematics and Physics "Ennio De Giorgi", University of Salento, Via Arnesano, Lecce, LE 73100, Italy
[b] Institute for Microelectronics and Microsystems (IMM), CNR, Via Monteroni, Lecce 73100, Italy
[c] Department of Experimental Medicine - University of Salento Centro Ecotekne, S.P.6, 73043 – Monteroni, Lecce 73100, Italy
[d] Institute of Science of Food Production, C.N.R. Unit of Lecce, Lecce 73100, Italy

ARTICLE INFO

Keywords:
Green synthesis
Gold Nanoparticles
Polyphenols
Inflammatory responce
Morphomechanical changes

ABSTRACT

Green synthesis from plant waste involves the generation of functional nanoparticles (NPs), offering significant potential for a wide range of applications. Numerous studies have focused on the use of plant extracts to produce AuNPs suitable for various applications in the medical field, particularly in photothermal therapy and cancer therapy, owing to their plasmonic properties. Moreover, NP-mediated immunostimulation and immunosuppression is an intriguing field of research, focusing on how manipulation of NP physicochemical properties can influence their inter-action with immune cells and immune modulation. However, to date, few investigations have been conducted on the modulation of the inflammatory response mediated by green-synthesized nanostructures. To this aim, we synthesized AuNPs using extracts of *Laurus nobilis*, which exhibit high crystallinity and are inherently coated by a dense network of polyphenols, thus maintaining stability on their surface through the green synthesis approach. Then, in order to explore how these green-synthesized nanostructures can enhance or suppress the inflammatory cellular responses, we investigated the response of free polyphenols and AuNPs@polyphenols in murine bone marrow derived dendritic cells (BMDCs), by means of morphomechanical analysis and biochemical assays. Our findings demonstrated that DCs exposed to both free polyphenol extract and AuNPs@polyphenols were able to inhibit the secretion of crucial inflammatory mediators in response to lipopolysaccharide (LPS) administration. Therefore, polyphenols immobilized on Au surface were more effective in the inflammation suppression. These evidence paving the way for a powerful strategy to develop edible anti-inflammatory adjuvants, overcoming the limitations associated with the use of free polyphenols in clinical practice.

Introduction

The field of green chemistry, established by the Environmental Protection Agency (EPA) two decades ago, has arisen in response to the escalating demand for environmentally sustainable practices within the chemical industry [1]. Its primary goal is to decrease or exclude the use of harmful substances and minimize or prevent the generation of waste in chemical reactions, while maintaining effectiveness [2]. A specific focus within this domain is devoted to nano-synthesis, which has garnered growing attention in recent decades. Notably, the production of plasmonic nanostructures from agricultural waste is of significant interest, with a focus on the reuse of biomass to create materials applicable in various fields [3,4]. Green synthesis from plant waste involves the creation of functional nanoparticles (NPs), offering significant potential for a wide range of applications in catalysis, sensing, electronics, photonics, and medicine, whose interest is significantly increased if the whole process is also considered from a circular economy perspective [5,6]. Different noble metals NPs can be obtained by means of these synthesis processes, since plant extracts enables the utilization of molecules inherently present in different part of plants, employing a phytochemicals-driven approach [7–9]. In the specific case of Au, these agents encompass several reducing molecules such as antioxidants,

* Corresponding author at: Department of Mathematics and Physics "Ennio De Giorgi", University of Salento, Via Arnesano, Lecce, LE 73100, Italy.
E-mail address: ross.rinaldi@unisalento.it (R. Rinaldi).

https://doi.org/10.1016/j.nantod.2024.102329
Received 10 December 2023; Received in revised form 3 May 2024; Accepted 27 May 2024
Available online 31 May 2024

enzymes, and phenolic moieties, able to facilitate the reduction of gold cations from $HAuCl_4$ into gold NPs (AuNPs). This process further prevents the aggregation of Au atoms into nanoscale particles, ultimately stabilized by the phytochemicals to yield isotropic AuNPs [10,11].

The capping of polyphenols on the surface of the NPs is particularly intriguing [12]. These polyphenols act to shield the nanostructure, thereby ensuring the colloidal solution of these NPs remains stable in an aqueous solution [13]. Numerous studies have focused on the use of plant extracts to produce AuNPs for various applications, particularly photothermal therapy and cancer therapy due to their plasmonic properties [14]. Moreover, NP-mediated immunostimulation and immunosuppression is an intriguing field of research, focusing on how manipulation of particle physicochemical properties can influence their inter-action with immune cells and immune modulation [15,16]. However, to date, limited investigation has been conducted on the modulation of the inflammatory response, specifically examining how these green-synthesized nanostructures can enhance or suppress the inflammatory cellular responses.

In literature, there is comprehensive documentation highlighting the capacity of polyphenols to skew inflammation towards tolerance [17–19]. These compounds serve as exogenous potent antioxidants against oxidative stress induced by high levels of reactive oxygen species (ROS), thereby preventing apoptosis and necrosis [20]. Importantly, they assume a pivotal role in conferring cardioprotective and anticancer properties, coupled with the ability to modulate enzymes implicated in the onset of pathological conditions [21,22]. Despite these noteworthy advantages, polyphenols present high susceptibility to heat and light, limited water solubility, high metabolic rates, and swift elimination from the body [23]. These factors collectively contribute to their poor stability and bioavailability of polyphenols, thereby significantly diminishing their efficacy. This underscores the critical nature of polyphenol applications in clinical practice [24].

In this scenario, our work is focused on green synthesis of AuNPs that serve as vector to polyphenols to overcome the clinical issues related to free polyphenols use in therapeutic applications. Specifically, in this study we synthesized AuNPs utilizing extracts of *Laurus nobilis*, a plant typical of the Mediterranean flora and known for its various therapeutic properties. Indeed, *Laurus nobilis* leaves contain several phenolic compounds, including flavonoids, phenolic acids, tannins (proanthocyanidins), and lignans. Surprisingly, we achieved simultaneously different AuNPs shapes, nanospheres and two-dimensional nanotriangles, having highly crystallinity. In addition, these nanostructures appeared covered by a dense network of polyphenols that remain stable on the surface (AuNPs@polyphenols). Comprehensive characterization of morphology with high resolution, surface charge and elements composition were conducted using Transmission Electron Microscopy (TEM), high-angle annular dark-field Scanning Transmission Electron Microscopy (STEM-HAADF), ζ potential, UV–vis spectroscopy, and Energy-Dispersive X-ray Spectroscopy (EDS).

Subsequently, we investigated the response of free polyphenols and AuNPs@polyphenols in murine bone marrow derived dendritic cells (BMDCs), particularly by a morphomechanical perspective. The correlation between inflammation and membrane elasticity is of significant interest in biomedical research [25]. Precisely, membrane elasticity denotes the ability of a cell membrane to deform and return to its original shape. This characteristic is crucial for numerous cellular functions, including the response to mechanical forces and the flexibility necessary for adhesion, motility, and cell division. In the presence of inflammation, the reorganization of the cytoskeleton can occur, influencing the mechanical response of cell membrane and affecting its elasticity. In particular, dendritic cells (DCs) antigen presenting ability requires high deformability to sustain migration towards lymph nodes and stable and prolonged adhesion with T cells. [26,27] These effects serve a notable indicator for characterizing the response of dendritic cells to heightened levels of inflammation; this correlation is consistently supported by several studies. Notably, these changes have been demonstrated to be associated with the migration towards lymph nodes and, in turn, to the regulation of immune defense and homeostasis, further emphasizing their relevance in understanding dendritic cell behavior [28]. In this aim, we have evaluated the F-actin rearrangement by means high resolution confocal fluorescence microscopy (CLSM) and correlate the reorganization of cortical cytoskeletal network with the indentation measurements performed in living condition through Atomic Force Microscopy (AFM).

Our findings demonstrated that, *in vitro*, DCs exposed to both free polyphenol extract and AuNPs@polyphenols were able to suppress the secretion of crucial inflammatory mediators in response to LPS administration.

Taken together, these data suggest that the utilization of AuNPs derived from *Laurus nobilis* leaves via green synthesis represents a potent strategy for developing edible anti-inflammatory adjuvants, overcoming the limitations associated with the clinical use of polyphenols.

Materials

Extraction of leaf components

During the winter season, leaves from the *Laurus nobilis* plant were gathered. Following multiple rinses with MilliQ water to eliminate impurities, the leaves were air-dried at room temperature for 24 h. Subsequently, 25 g of the dried leaves were finely chopped and introduced into a beaker containing 250 mL of MilliQ water. The mixture underwent boiling at 100 °C for 20 min, followed by gradual cooling to room temperature. Prior to utilization in the NPs synthesis, the extract underwent filtration using Whatman No. 1 filter paper. For cellular incubation, the solution underwent sterilization through a freeze-drying process.

Environmentally friendly synthesis of gold nanoparticles (AuNPs)

Initially, 5 mL of the refined leaf extract was combined with a solution containing $HAuCl_4$ dissolved in MilliQ water (1 mM), maintaining a 1:4 ratio between the extract and the $HAuCl_4$ water solution. The amalgamation was subjected to stirring at 300 rpm for 1 h at room temperature, resulting in a color change of the reaction solution from light brown to wine red. The solution underwent centrifugation for 1 h at 4000 rpm to collect the NPs in the pellet, which was subsequently purified with MilliQ water through three cycles of centrifugation. Ultimately, the NPs were concentrated using an Amicon Ultra Centrifugal 3k Filter (Sigma Aldrich, Dorset, UK).

UV–vis spectroscopy

The surface plasmon responses of different AuNPs@polyphenols were recorded using a Shimadzu-2550 with 1 cm quartz cuvettes.

ζ-potential

The ζ-potential acquisitions were recorded by a Zetasizer Nano-ZS, with a HeNe laser (4.0 mW) working at 633 nm detector (ZEN3600, Malvern Instruments Ltd., Malvern, UK), in aqueous solutions (25 °C, pH 7).

NPs concentration

The concentrations of the AuNPs@polyphenols were calculated by elemental analyses using an ICP-OES Perkin Elmer AVIO 500. A total of 200 μL of the AuNPs solution was digested overnight by adding 2 mL of aqua regia (HCL:HNO_3, 3:1), followed by dilution with MilliQ water (1:5).

Total polyphenol content determination

The total polyphenol content was determined spectrophotometrically according to the Folin-Ciocalteu method [29]. Briefly, 50 microliters of gallic acid standard or samples, and 50 microliters of Folin-Ciocalteu Reagent (Sigma-Aldrich) (1:5, v/v) were placed in each well of a 96 well-plate, then 100 μL of sodium hydroxide (0.35 M) was added. The absorbance of blue complexes was monitored at 760 nm after 5 min and it was compared with that of a gallic acid standard curve ($R\ 2 \geq 0.997$). Total polyphenol content was then expressed as gallic acid equivalents (GAE) $mg \cdot g^{-1}$ of dry weight (DW) [30].

Atomic scanning transmission electron microscopy (ASTEM) high angular annular dark field (HAADF) and bright field (BF)

Atomic resolution images and bright field images were obtained in a JEOL NEOARM200F HOLO-TEM microscope equipped with spherical aberration, image e spectrum correctors (ASCOR/CESCOR) capable of correcting aberrations up to the 5th order and operated at 200 kV. The microscope is also equipped with two EDS (energy dispersive x-ray detectors) and with an EELS (energy dispersive electron energy loss spectrometers). The image resolution was demonstrated to be lower than 1 Å.

Mice

Animal studies were conducted in accordance with national and international guidelines and were approved by the authors' institutional review board (Organism for Animal Wellbeing—OPBA). All animal experiments were carried out in accordance with Directive 86/609 EEC enforced by Italian D.L. n. 26/2014 and approved by the Italian Animal Ethics Committee of Ministry of Health—General Directorate of Animal Health and Veterinary Drugs (Authorization n° 1069/2020-PR, 04–11–2020). Wild-type C57BL/6 mice (Stock No.: 000664; weight: approximately 20 g).

Culture and treatment of murine bone marrow derived dendritic cells (BMDCs)

BMDCs were obtained from 16-week-old male C57BL/6 J mice. Briefly, a single cell suspension of BMDCs precursors was obtained by flushing the tibiae and femurs with 1X D-PBS (Gibco, New York, NY, USA) in which 0.5 mM EDTA (Thermo Fisher Scientific, Waltham, MA, USA) was added, followed by hypotonic lysis of red blood cells with ACK (Ammonium-Chloride-Potassium, Thermo Fisher Scientific, Waltham, MA, USA) lysing buffer. BMDCs precursors were plated in a 10 mL dish (1×10^6 cells/mL) and cultured in RPMI-1640 (Thermo Fisher Scientific, Waltham, MA, USA) enriched with 10 % heat-inactivated fetal bovine serum (FBS, Thermo Fisher Scientific, Waltham, MA, USA), 100 U/mL penicillin and 100 mg/mL streptomycin (Thermo Fisher Scientific, Waltham, MA, USA), 25 μg/mL rmGM-CSF and 25 μg/mL rmIL-4 (Miltenyi Biotec, Bergisch Gladbach, Germany) at 37 °C in a humidified 5 % CO_2 atmosphere. On day 3, the cells were harvested, restimulated with 25 μg/mL rmGM-CSF and 25 μg/mL rmIL-4, and plated at 1×10^6 cells/mL in a 10 mL dish. On day 8, the cells were harvested plated at 1×10^6 cells/mL on a 12-well culture plate. The cells were treated with 10 μM of AuNPS binding *Laurus nobilis* extracts or only leaves extract prepared from the indicated cultivar. After 24 h, cells were stimulated with 1 μg/mL of Salmonella Typhimurium LPS (Sigma-Aldrich, St. Louis, MO, USA).

Then, 6 h later, cells were harvested to proceed with RNA extraction, while for the ELISA assay and microscopy, LPS treatment was stopped after 24 h. Subsequently the supernatant was collected and used for cytokines detection.

Transmission electron microscopy (TEM) for cell uptake visualization

Cell samples were rinsed, fixed using 2.5 % glutaraldehyde, then post-fixed with 1 % osmium tetroxide containing 1.5 % potassium cyanoferrate. Afterward, the cellular monolayers were gradually dehydrated in ascending concentrations of ethanol and embedded in Epon resin. Thin sections of 80 nm were obtained using an ultramicrotome and collected onto copper TEM grids. The grids were finally doubly stained by lead citrate and UranyLess EM Stain (Electron Microscopy Sciences), by following the standard protocol provided by the manufacturer. TEM analysis was performed with a JEOL JEM-1011 transmission electron microscope at 100 kV operating voltage, equipped with a 7 megapixel CCD camera (Orius SC600A, Gatan, Pleasanton, CA). TEM image analysis was achieved with Gatan Digital Micrograph™ (DM) software.

Viability test

BMDCs were seeded at a concentration of 1×10^6 cells per well in 12-well plates (Thermo Fisher Scientific). in a humidified atmosphere, with 95 % air and 5 % CO_2, at 37 °C. Control wells were incubated with equivalent volumes of a cell culture medium. The cells were exposed to AuNPs@polyphenols for 24 h and then to LPS for 24 h. The same procedure was used to quantify the viability of using plant extract. MTT (0.5 mg/mL) was added to the cells for a 3 h incubation and cells were lysed in acidified isopropanol/HCl 0.04 N. The lysates were subsequently read on a spectrophotometer at 550 nm (Bio-rad, Richmond, CA, USA). The results were calculated as percent viability compared to control.

Analysis of cytokine secretion

Cytokine secretion of coculture supernatants was analyzed using ELISA kits for IL-1α, IL-1β, IL-10 and TNF (R& D Systems, Minneapolis, MN, USA Catalog #: DY400, DY401, DY417 and DY410 respectively) on cell culture supernatants from 3 independent experiments following the manufacturer instructions,.

Confocal microscopy

BMDCs cells were seeded at a concentration of 7×10^4 cells/mL in glass Petri dishes (Greiner Bio-One GmbH, Kremsmünster, Austria), After 24 h of stabilization, cells were treated as described in 2.10 section. The culture media with different treatment condition was removed, and the cells were gently washed with PBS. The samples were fixed using glutaraldehyde (0.25 %) for 10 min, and then the cells were permeabilized by Triton X-100 (0.1 %) for 5 min. The actin fibers were stained using 1 μg/mL of phalloidin-FITC overnight whereas nuclei were labelled with DAPI (1 ug/mL). The high-resolution fluorescence acquisitions were performed on a Zeiss LSM700 (Carl Zeiss Microscopy, Munich, Germany) mounted on an Axio Observer Z1 (Carl Zeiss Microscopy, Munich, Germany) inverted microscope, using the Alpha Plan-Apochromat (Carl Zeiss Microscopy, Munich, Germany) 63x oil-immersion objective having nominal NA equal to 1.46 (Carl Zeiss Microscopy, Munich, Germany).To visualize nuclear chromatin marked with DAPI and cytoskeletal actin proteins stained with phalloidin-FITC was employed lasers with λ_{ex}= 405 nm and λ_{ex}= 488 nm, and the aperture of pinhole was maintained at 1,88 and 1,58, respectively, were used. The acquisitions were acquired in sequential mode of two laser, to optimize the quality of emission signals. In addition, all measurements were obtained while keeping the acquisition parameters constant as follows: image size (203,23 μm * 203,23 μm), gain 700, digital gain 1.2, digital offset -70 for channel correspondent to λ_{ex}= 405, and gain 615, digital gain 1.2, digital offset-70 for channel correspondent to λ_{ex}= 488 nm. The image resolution has been set at 1024 pixels * 1024 pixels for acquisition in z-stack mode.The confocal acquisitions were analyzed

by ZEN2010 software (ZEISS, Germany) and cytoskeletal coherency quantifications were performed on 15 cells for each treatment, using the ImageJ 1.51 p analysis software, using OrientationJ plugin [32]. Data were expressed as mean value and their relative standard deviation.

AFM analysis

High-resolution Atomic Force Microscopy NTEGRA (NT-MDT Spectrum Instruments, Moskow, Russia) was employed to investigate the morphology and stiffness of the samples. In particular, the morphological analysis was performed by using NSG01 probes (NT-MDT Spectrum Instruments, Moskow, Russia). These probes are characterized by a tetrahedral shape with a typical tip curvature radius less than 10 nm, and a tip cone angle less than 20°. The tip is mounted on the apex of a rectangular single-crystal silicon cantilever with a thickness of 1.25 μm, a nominal spring constant and resonant frequency equal to 5.1 N/m and 150 kHz, respectively. The topographic acquisitions were taken in Semi-contact error mode, over areas of 50 μm × 50 μm with a resolution of 512 points × 512 points, setting the setpoint, gain and rate parameters to about 6.1 nA, 2.34, and 0.5 kHz, respectively. Each topographical image was digitally treated with a plane fit and with a second order flattening to suppress bow and tridimensionality effects, using specific tools of acquisition software Image Analysis P9 (NT-MDT Spectrum Instruments, Moskow, Russia). To quantify the cells elasticity force indentation experiments were performed in cellular living condition, using a proper tip holder for the analysis of samples in liquid medium. The curves were acquired by using CSG01 probes (NT-MDT Spectrum Instruments, Moskow, Russia) that consist of a high-sensitivity rectangular cantilever having a tetrahedral tip at its free end. The tip cone angle is less than 22°, curvature radius is equal to 10 nm. The nominal resonant frequency and elastic spring constant indicated by the manufacturer amount to 9.81 kHz and 0.03 N/m, respectively. Prior to performing the force-spectroscopy measurements, the spring constant of CSG01 cantilevers was accurately estimated via the thermal noise method [31]. The approach data portion of indentation curves was fitted by using the Sneddon model and then Young's Modulus (E) values were obtained as the best fit parameter. More in detail, for each sample, the E was calculated as the average value on 100 curves, randomly acquired on 10 different cells. All measurements were performed in ambient conditions (room temperature of about 25 °C and relative humidity of around 55 %. The analysis of indentation curves was carried out using the Image Analysis P9 (IA-P9) software (NT-MDT Spectrum Instruments, Moskow, Russia).

Data analysis

All experimental data were analyzed and plotted by using Origin Pro v8 (Origin-Lab Corporation, Northampton, MA, USA). Data were considered statistically significant for p-value (t-student or ANOVA test) less than 0.05.

Results and discussion

Green chemistry has emerged as a highly relevant topic in the field of nanotechnology. The ability to harness plant-derived products for the creation of nanostructures exhibiting several applications and specific physicochemical properties is garnering increasing attention [32]. The biomedical domain demonstrates substantial interest, given that the elimination of toxic agents employed in nanostructure synthesis enables to produce nano-objects with markedly low toxicity [11,33]. Whitin this context, numerous publications have focused on the use of plant extracts to obtain metallic NPs in varying sizes [34]. However, regarding the shape, the literature currently lacks sufficient evidence of accurate shape control. Consequently, many syntheses appear to be semi-spherical and polydisperse [33].

On the contrary, our work yielded two distinct forms of AuNPs in the single synthesis, specifically spherical and triangular, by employing *Laurus nobilis* extract, as showed in Fig. 1. Notably, Fig. 1**a** and 1**b** presented TEM acquisitions at two different magnifications, clearly showcasing both forms of achieved NPs. Spherical NPs showed a notably high density, as indicated by the pronounced contrast. Conversely, triangular NPs exhibited a different contrast, signifying their bidimensional nature as Au nanosheets. Fig. 1**c** and 1**d** depicted morphological analysis using STEM acquisitions in bright field and HAADF-STEM respectively. Gaussian fit of size distribution analysis unveiled distinct sizes of the two populations of NPs. Spherical AuNPs exhibited a size of (40 ± 6) nm, while triangular AuNPs@polyphenols showcased a larger size, equal to (180 ± 6) nm.

Employing high-resolution microscopy, the presence of an evident shell enveloping the two types of NPs was observed (Fig. 2**a**). This shell was readily discernible due to its distinct contrast compared to Au (Fig. 2**b, c**). To affirm that this capping was indeed the result of the presence of polyphenols on the surface, we conducted an EDS analysis. This latter confirmed the presence of both elements: Au and carbon. In this regard, the detected carbon was attributed to the organic shell of polyphenols, characterized by long carbon chains (Fig. 2**d, e, f, g**).

The UV-Vis spectra of AuNPs@polyphenols revealed an absorption peak at approximately 555 nm, while the plant extracts presented absorption around 260 nm, due to the phenolic compounds (Fig. 3**a**). In the UV-spectra of AuNPs@polyphenols a subtle shoulder around 260 nm was observed, confirming the interaction of the polyphenols with the surface of AuNPs. In addition, the surface charge measurement by ζ potential indicated a negative charge, specifically (-34 ± 5) mV (Fig. 3**b**), attributed to the presence of hydroxyl groups.

The utilization of TEM for assessing the NPs uptake was conducted to assess the mechanisms of endocytosis involving AuNPs@polyphenols. TEM captures images using a stream of electrons that passes through a thin specimen, enabling a thorough examination of the sample's interior. This microscopy technique has found widespread application in nanomedical research, unveiling intricate connections between NPs and cellular or tissue components owing to its exceptional high-resolution capabilities. The remarkably short wavelength of the electron beam, which is 100,000 times shorter than photons in the visible spectrum, allows for sub-nanometer resolution, roughly equivalent to 0.2 nm in conventional TEM.

TEM can offer clear insights into the mechanisms through which NPs enter cells by traversing the plasma membrane, provided that the sample has been appropriately processed to maintain its spatial relationship with the cell surface. This understanding is highly valuable for the development of effective delivery systems.

We conducted an analysis of the AuNPs@polypehnols internalization in cells by TEM imaging after 24 h. Fig. 4 **a** and **b** displayed the typical morphology of dendridic cells, characterizedby round body with irregular dendritic like projections. Fig. 4**c, d** showed cells incubated with AuNPs@polyphenols, while cells exposed to AuNPs and LPS were represented in Fig. 4 **e, f**. Notably, no discernible differences were observed between the two sample conditions in the internalizaton process.

Endocytosis can occur for both individual NPs and small groups of NPs; larger single nanoconstructs or clusters of AuNPs@polyphenols, on the other hand, may enter cells through phagocytosis or macropinocytosis, respectively. The predominant uptake mode was endocytosis, where the NPs after cell membrane contact, entering the cell. In our case, the two different shapes of NPs were presumably internalized by the clathrin-mediated endocytic pathway or, in the case of triangular shapes, by cytoskeletal rearrangement [35,36]. The AuNPs@polyphenols were found concentrated within vacuoles (namely, endosomes and/or lysosomes) in the perinuclear region of the cells, with no presence detected within the nucleus and without difference from size and shape.

Dendritic cells exposed to polyphenols lose the ability to become inflammatory even if exposed to one of the most potent inflammatory stimuli, the TLR4 ligand LPS [37,38]. We used in vitro cultured murine

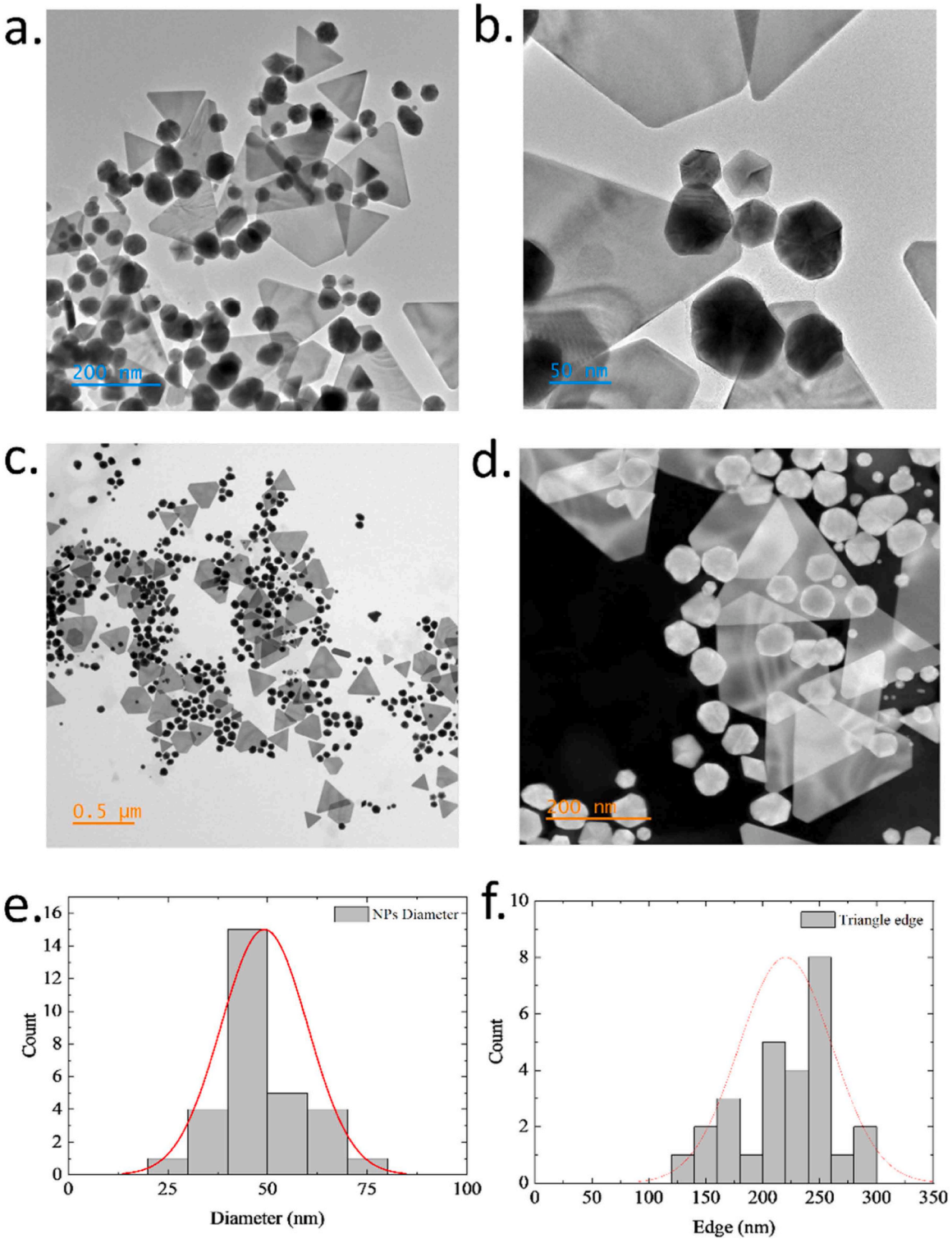

Fig. 1. Representative TEM images of AuNPs@polyphenols at different magnifications (a, b). Representative STEM acquisitions bright field (c) and HAADF-STEM (d). Statistical analysis of NPs size calculated by ImageJ software on 70 NPs. Red line is the Gaussian fit.

DCs to evaluate if the interaction of the polyphenols with the surface of AuNPs altered polyphenols ability to suppress the inflammatory pathway induced by LPS. We exposed murine bone marrow derived dendritic cells (BMDCs) to AuNPs@polyphenols for 24 h before receiving LPS administration to induce DCs maturation.

We first addressed DCs viability up to 96 h following AuNPs administration by MTT. None of the different concentrations of AuNPs@polyphenols (10, 20 and 40 μM) or *Laurus nobilis* extracts (2, 4 and 8 μg/mL) affected DCs viability (data not shown) as also reported in our previous publications using different immunocells, i.e THP-1 [39]. Of note, we tested AuNPs@polyphenols carrying different ratios of polyphenols to NPs to evaluate whether the eventual biological effect was due to the NPs or the polyphenol component. DCs switch from the immature (iDCs) to mature (mDCs) status is typically a consequence of the engagement of pathogen-associated molecular patterns (PAMPs) such as toll-like receptor (TLRs). In response to LPS administration DCs

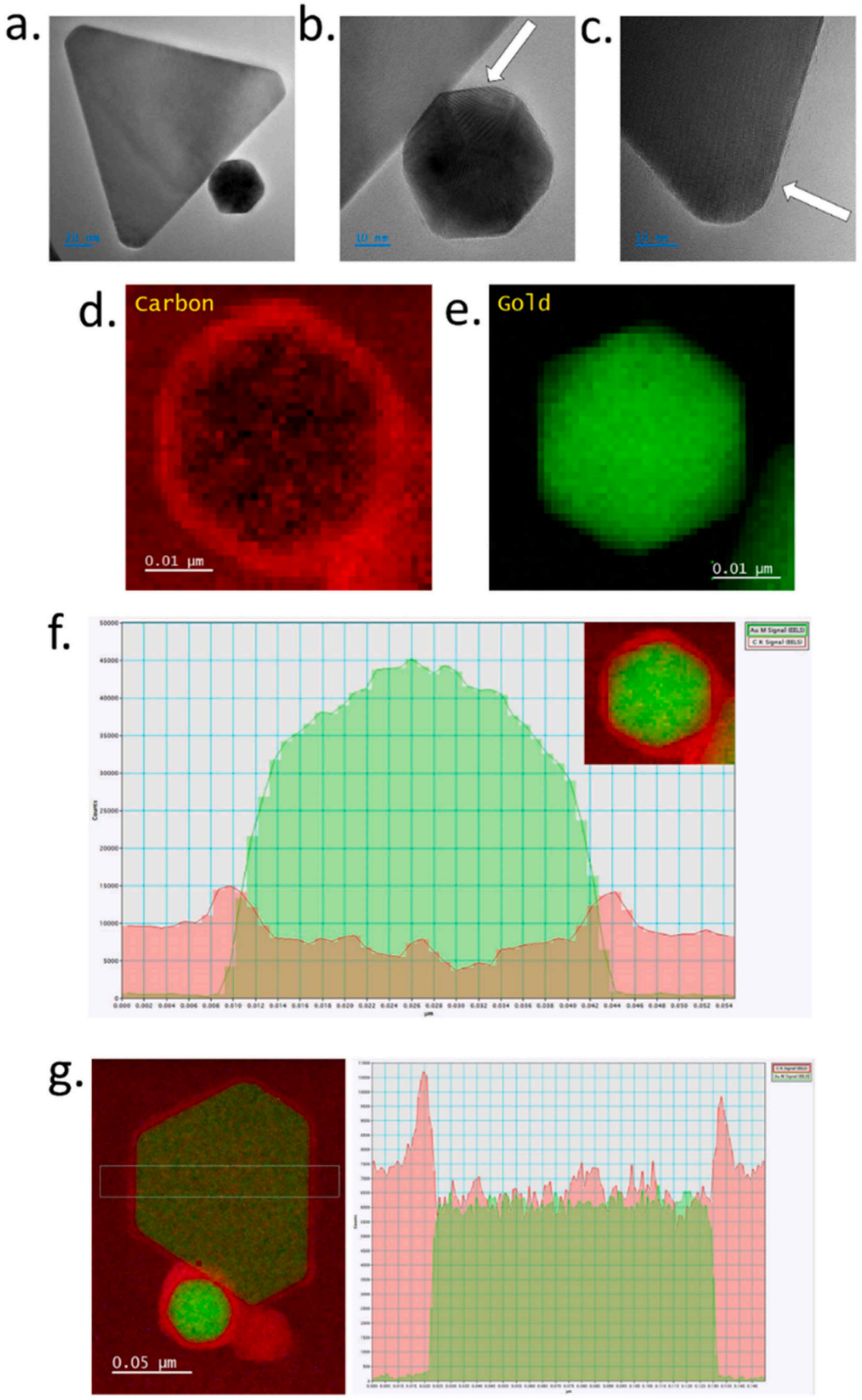

Fig. 2. Representative STEM bright field images of AuNs@polyphenols (a). In b and c details of the two shapes of NPs were reported in which was visible the organic shell. EDS images (d,e) and analysis (f,g) of AuNPs@polyphenols.

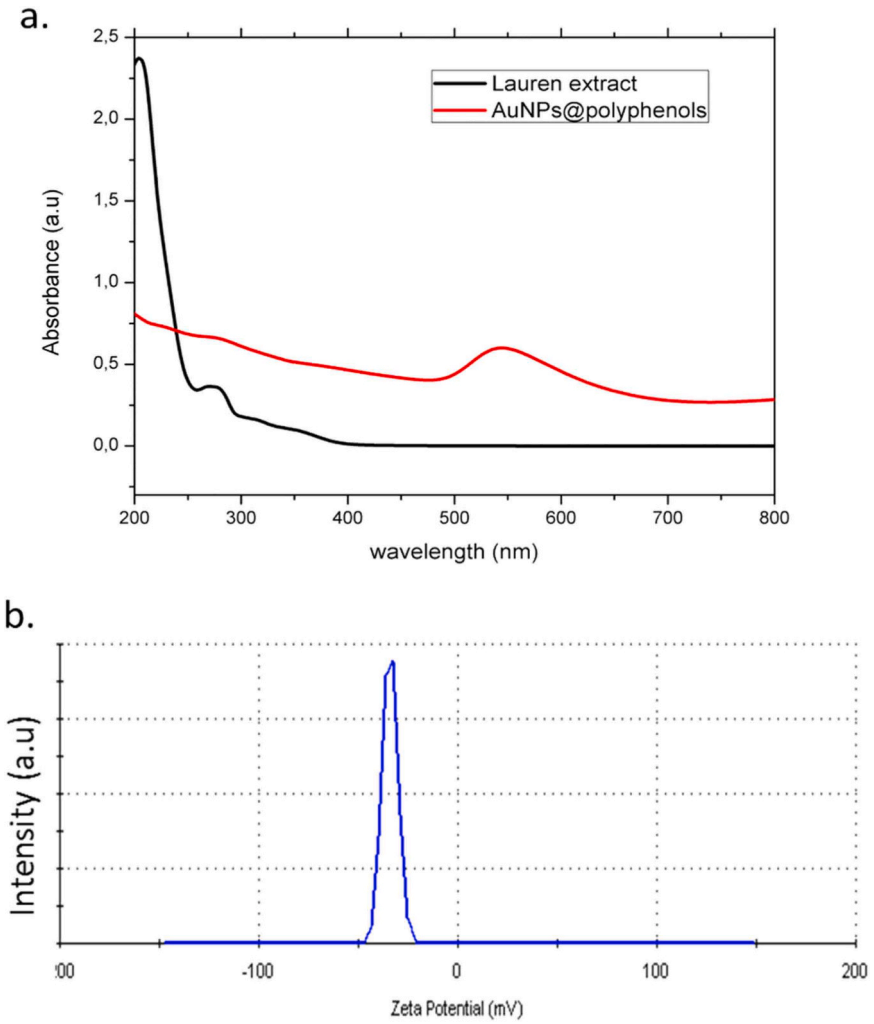

Fig. 3. Uv-vis spectra of *Laurus nobilis* extract (black line) and AuNPs@polyphenols (red line) (a); zeta potential measuements of AuNPs@polyphenols (b).

profoundly change their phenotype, morphology and cytokine secretion profile becoming mDCs [40,41].

Exposure to polyphenols can change DCs maturation towards an inflammatory-impaired phenotype characterized by low inflammatory cytokine secretion, migration towards draining lymph nodes and distinct gene transcription profile [42,43]

To evaluate if bending to AuNPs@polyphenols preserved polyphenol ability to skew DCs inflammatory response following LPS administration we exposed cells to AuNPs@polyphenols for 24 h and then administered LPS.

Cytokine concentration in the supernatant revealed that the administration of AuNPs@polyphenols [10 μM - 8 μg/mL polyphenols] was able to significantly reduce IL-1α, IL-1β and IL-10 secretion, but not TNF (Fig. 5).

Depending on the initial concentration in the *Laurus nobilis* extract used for the synthesis process, different coverage of polyphenols onto the AuNPs can be obtained and carefully quantified, as described in Section 2.

Increasing concentrations of AuNPs@polyphenols [20 μM-8 μg/mL polyphenols and 40 μM-8 μg/mL polyphenols] were not able to further reduce IL-1α and IL-1β secretion [29], suggesting that the reduction of the inflammatory cytokines' secretion was due to the labeled polyphenols and unrelated with AuNPs. The ELISA analysis confirmed that the TNF in response to LPS was not reduced by AuNPs@polyphenols [10 μM-8 μg/mL polyphenols], vice versa, IL-10 was efficiently suppressed suggesting that AuNPs@polyphenols act on specific inflammatory pathway. Importantly, the suppression of IL-10 transcription by means of AuNPs@polyphenols was strongly dependent on the concentration of the polyphenols in the surface shell, showing a suppression from about 50 % down to about 35 % by doubling the AuNPs@polyphenols [10 μM-8 μg/mL polyphenols and 20 μM-16 μg/mL polyphenols] further highlighting that the anti-inflammatory effect is mediated by the surface concentration of the polyphenols component independently from the amount of AuNPs@polyphenols carrier.

DCs ability to efficiently present antigens is strictly related with their ability to migrate to the draining lymph nodes and to create a stable synapse with naïve T cells [44,45], thus profound morphological and phenotypical differences distinct iDCs from mDCs. A round and smooth surface in iDCs becomes rough surface with multiple pseudopodia in mDCs [46]. To assess whether AuNPs@polyphenols can express their anti-inflammatory ability by preventing the phenotypical maturation of DCs, we visualized DCs morphology, in terms of nuclear and cytoskeletal, by confocal microscopy. In Fig. 6, a multi-panel of 3D images related to the samples was presented. In particular, the control samples (Fig. 6**a**) exhibited a typical morphology, characterized by smooth surface with few protrusions. A similar appearance was observed in cells incubated with *Laurus nobilis* extract. (Fig. 6**b**). Conversely, following LPS inoculation for 24 h, cells differentiated into a typical inflammatory morphology, indicating their probably phenotypical maturity (Fig. 6**c**).

In more detail, IDCs typically remained non-migratory and stationary in peripheral tissues, awaiting encounters with pathogens and foreign materials. The phagocytose of foreign molecules trigger their

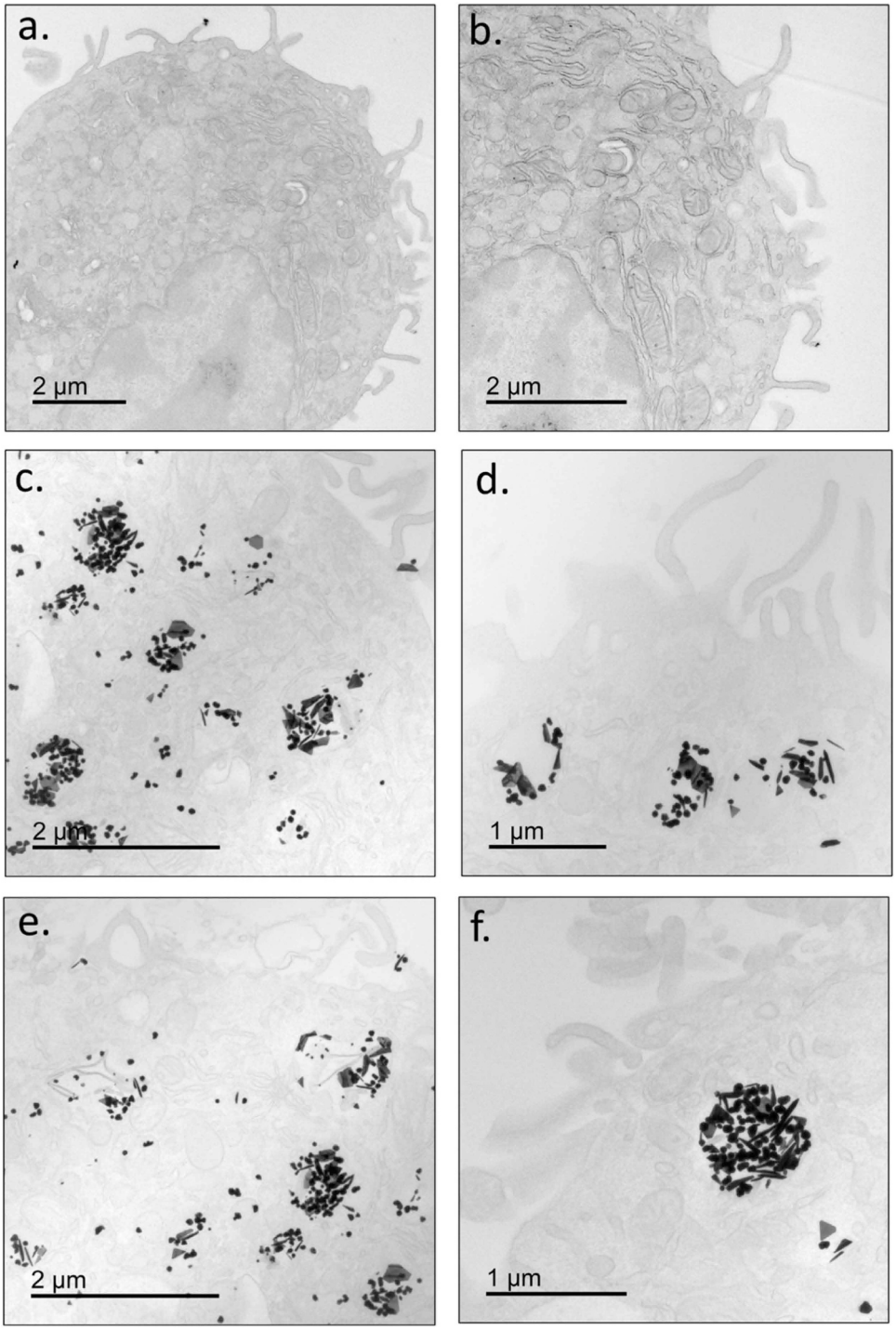

Fig. 4. TEM images at different magnification of BMDCs control (a,b), loaded with AuNPs@polyphenols (c,d) and AuNPs@polyphenols + LPS.

maturation process, that involves a change in the morphology, leading to the formation of dendrites and pseudopodia. During the transformation, the chemotactic activities of mDCs and the capability of migration increases.

The mDCs, both phenotypically and functionally, initiate migration in response to chemokines released from the lymph nodes. These mature DCs then engage with naive T cells [47]. The maturation process involves a change in the morphology of DCs, leading to the formation of dendrites and pseudopodia. During this transformation, the chemotactic activity of DCs is heightened through the expression of actin-bundling proteins that facilitates the assembly of membrane protrusions, thereby enhancing cell migration [48].

Exposing cells to AuNPs@polyphenols induced a phenotype similar to both control cells and cells treated with *Laurus nobilis* extract and LPS. The inflammatory phenotype appeared to be reduced (Fig. 6**d**), and the effects became more pronounced when AuNPs@polyphenols were incubated with LPS. (Fig. 6**e**). Consequently, based on this analysis we may conclude that the AuNPs@polyphenols were more effective in reducing inflammation through a morphological point of view.

On average, DCs did not exhibit a particularly organized cytoskeleton; actin filaments were rather randomly arranged. However, the analysis of the coherency parameter enables the quantification of subtle

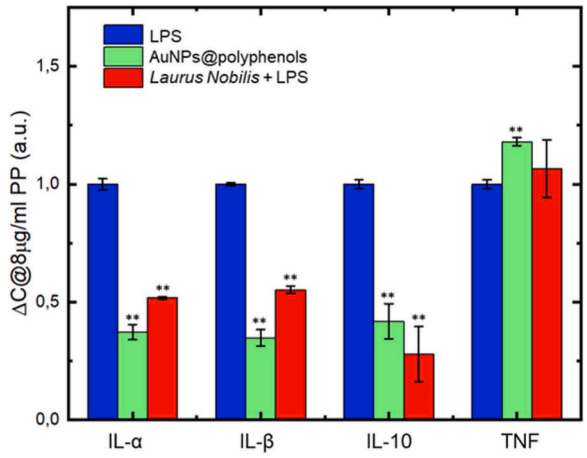

Fig. 5. Histograms expressing the reduction of the mean concentration ΔC (±SD; n=3) assessed by ELISA for secreted cytokines of BMDCs after stimulation with LPS and/or Au@polyphenols, free polyphenols from *Laurus nobilis* extract. Data are statistically significant for *p < 0.05 **p < 0.005 . The original measured values (ng/mL) were normalized to the maximum concentration of expressed cytokines, which was always observed after stimulation with LPS, which was set equal to 1.

variations in the organization of these filaments. The coherency parameter expresses the local orientation of actin fibers: more disordered fibers showed values close to 0, whereas perfectly aligned ones showed a coherency value of about 1.

The quantitative assessment of coherency, conducted using the open-source tool specific to ImageJ software on confocal acquisitions, revealed a decrease in this parameter in cells stimulated with LPS, indicating a reduction in the organization of actin fibers. Conversely, cells exposed with AuNPs@polyphenols and LPS showed an increase in coherency values, due to the anti-inflammatory action of NPs, also in comparison to the *Laurus nobilis* extract and LPs alone (Fig. 6**f**).

It is known that immature dendritic cells (DCs) exhibit limited mobility; they are involved in environment screening and the capture of antigens within tissues or organs through processes such as phagocytosis or endocytosis [49]. The cytoskeletal rearrangement is crucial for immature DCs to engulf antigens effectively. However, upon maturation, DCs experience a reduction in phagocytic ability, an increase in motility, and exit the tissue [41]. They traverse the endothelium of lymphatic vessels and migrate towards draining lymph nodes. In these lymph nodes, mature DCs engage with T cells, initiating an adaptive immune response [50]. Then, a specific analysis of the mechanical behavior of these cells is fundamental to understand the role of polyphenols from extract and those bind on the AuNPs surface to support our hypothesis that AuNPs stabilize these fitomolecules improving their beneficial effects in cells. AFM analysis was performed on living cells (Fig. 7). Semicontact mode by in the height and error mode channel were showed. The morphology of control cells confirmed the data acquired by confocal microscopy. Cells control exhibited a predominantly round shape, with a quasi-smooth cell surface (Fig. 7**a**). In contrast, BMDCs stimulated with LPS (Fig. 7**b**) demonstrated an irregular shape characterized by numerous pseudopodia or lamellapodia, along with ridges and ruffles on the cell membrane surface. Additionally, they appeared slightly larger compared to the immature counterparts.

The addition of polyphenols from *Laurus nobilis* extract in cells exposed to LPS for 24 h reduced the quantity and the length of filopodia meaning the anti-inflammatory action of polyphenols (Fig. 7**c**). For cells exposed to AuNPs@polyphenols, we observed a control like morphology (Fig. 7**c**), whereas the incubation of dendritic cells with AuNPs@polyphenols and LPs induced an anti-inflammatory effect similar but stronger compared to cells exposed to free polyphenols and LPS (Fig. 7**d**).

Following this evidence, a meticulous analysis of Young's modulus on cortical actin was assessed across all experimental conditions, given the pivotal role of cytoskeleton as the physical and biochemical interface for a wide range of cellular processes [51]. Its intricate regulatory machinery is involved in both upstream and downstream aspects of numerous signaling pathways [52,53]. Playing a crucial role, the cytoskeleton governs the mechanical properties of a cell [54]. Consequently, cell elasticity may serve as a parameter reflecting the cellular behavior rather than representing the specific characteristics of isolated components [55]. In the context of BMDCs, it is reasonable to posit that single cellular mechanical phenotyping could offer biophysical insights into their inflammation process.

Therefore, AFM was employed as a powerful tool to understand the biophysical properties of cells [56]. Force-distance curves in correspondence of cells in living condition were acquired and analyzed to quantify their Young's modulus. Its value in control cells (Fig. 8**a**) corresponded to (3.9 ± 0.5) kPa; it became (2.4 ± 0.6) kPa after exposure to LPS for 24 h (Fig. 8**b**). This decrease may justifiable because BMDCs acquiring an inflammation phenotype were more capable to migrate. These results were corroborated by the analysis performed on the confocal images, from which resulted a reduced coherency value, corresponding to more disorganized actin fibers and in turn a cells elastic deformability. When NPs were expose to *Laurus nobilis* extract and LPS, the value of Young's modulus increased, becoming (2.9 ± 0.2) kPa. This may attribute to the presence of the polyphenols acting as anti-inflammatory agents (Fig. 8**c**). Incubation with AuNPs@polyphenols for 24 h did not show a significant alteration compared to control cells: specifically, Young's Modulus value resulted equal to (3.7 ± 0.8) kPa (Fig. 8**d**). Conversely, the addition of LPS of previous condition determined a decrease of the elastic modulus, that becoming (3.01 ± 0.8) kPa (Fig. 8**e**). This value was comparable with the cells exposed with free polyphenols.

In conclusion, considering the limitations related to the use on free polyphenols in medical applications, the use of green synthetized AuNPs@polyphenols may represent a promising solution, since polyphenols adhere and remain stable on the surface of the AuNPs overcoming the issue related to the very short half-lives of polyphenols. This is a crucial aspect of our work: we preliminary demonstrated how the use of AuNPs could imply the use of a much lower quantity of polyphenols to achieve the same therapeutic effect observed in free administration.

If confirmed in vivo, these data may support the translational use of AuNPs@polyphenols as adjuvant for drugs against chronic inflammatory syndromes, particularly Inflammatory bowel disease (IBDs).

Conclusions

Innovation in the nanomaterial field is addressing multiple challenges including the need of developing practices able to implement the biological effect of drugs and nutraceuticals and, at the same time, environmentally sustainable.

With the present study we describe a green one-pot synthetic process to obtain AuNPs@polyphenols obtained from the leaves of the *Laurus nobilis* extract.

Polyphenols are bioactive compounds able to suppress the anti-inflammatory pathway of immune cells. We recently used polyphenols as adjuvant for treatment of IBD in a single center study obtaining promising, but still unsatisfactory results [57]. Most likely, the effects of dietary polyphenols are limited by their poor stability and low availability.

The aforementioned results indicated that AuNPs@polyphenols retain the well know polyphenol ability to suppress the inflammatory pathway, furthermore, indicate that AuNPs@polyphenols captured by DCs enter in subcellular compartments and support an increase in coherency values in mDCs compared to AuNPs@polyphenols non-exposed one.

These are new and very interesting results as organelles are crucial

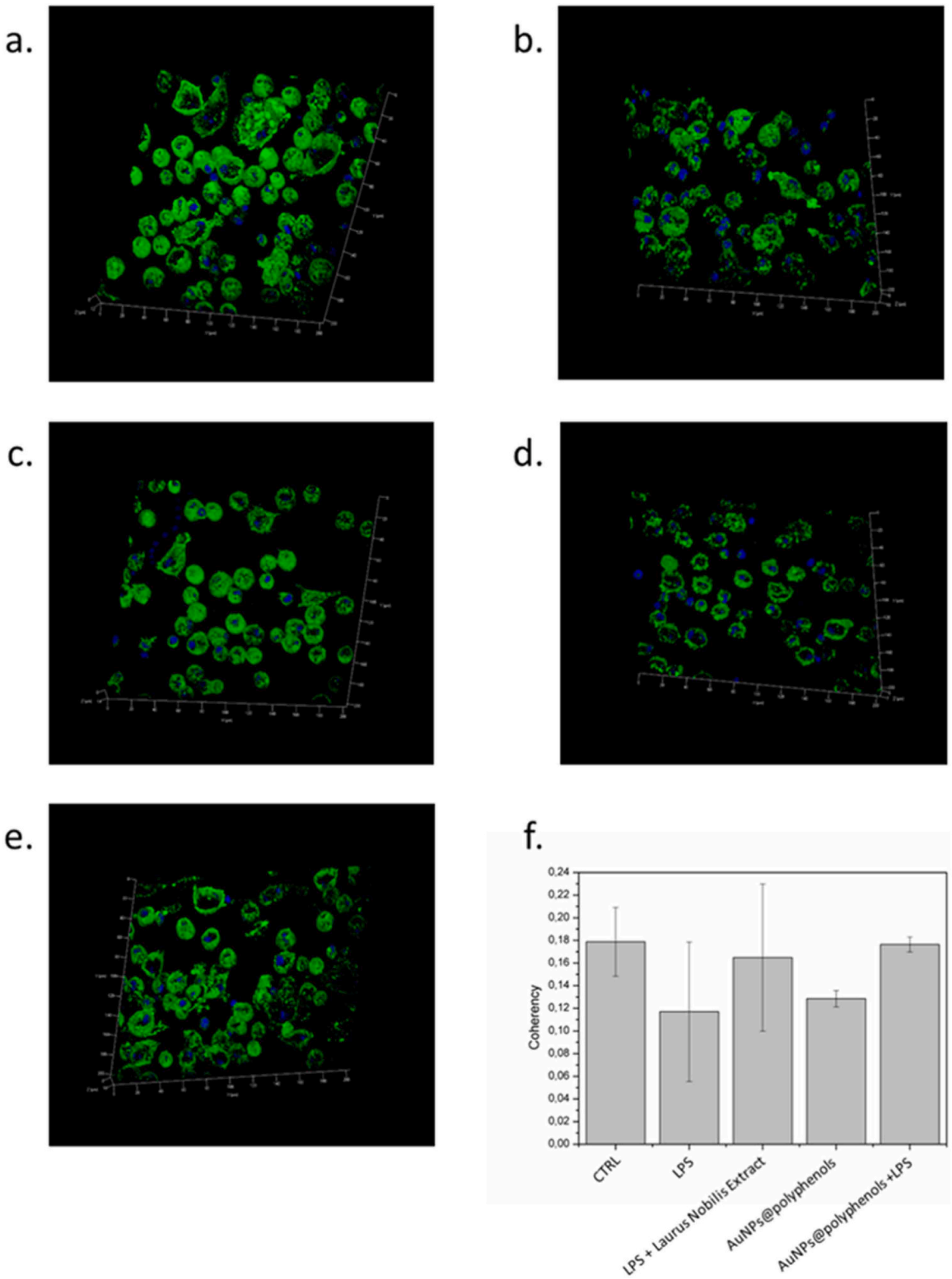

Fig. 6. . 3-d confocal acquisition z-stack of control (a), LPS (b), LPS and *Laurus nobilis* extract, AuNPs@polyphenols (c) and AuNPs@polyphenols and LPS (d). Coherency measurements on confocal acquisition using ImageJ software.

for antigen presentation and actin remodeling may indicate the possibility to prevent DCs migration towards draining lymph nodes.

In addition, the morphological and elasticity assessment of cortical actin of DCs cells showed that the addition of AuNPs@polyphenols in cells in which inflammation was inducted, reduced the cell stiffness. In particular, we demonstrated a reduction of inflammation more evident in the presence of AuNPs@polyphenols with respect to free polyphenols

CRediT authorship contribution statement

Marcello Chieppa: Supervision, Methodology, Data curation. **Angelo Santino:** Methodology, Data curation. **Rosaria Rinaldi:**

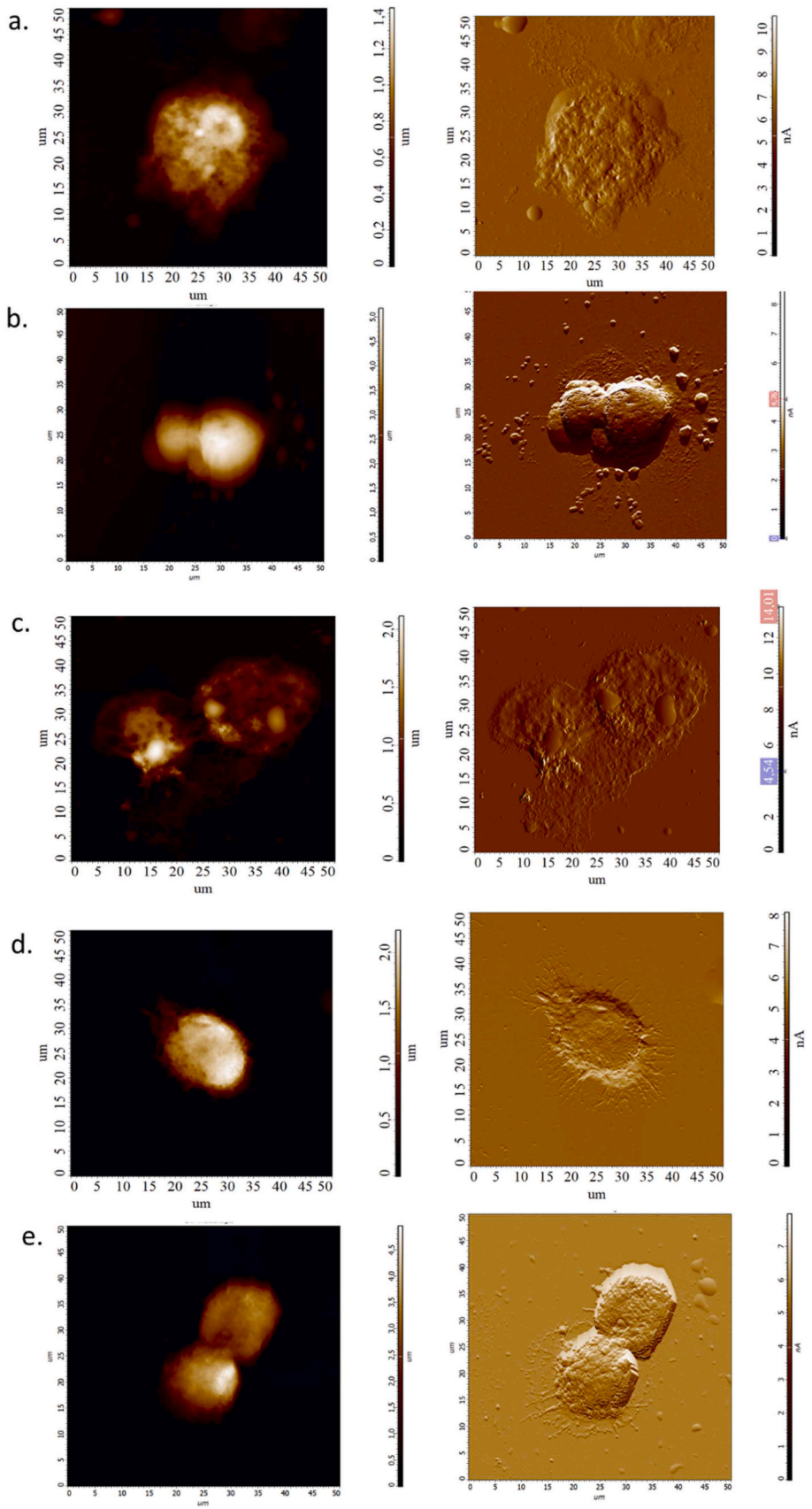

Fig. 7. Representative topographical acquisitions obtained in semicontact mode by atomic force microscopy in the height (left) and error mode (right) channel, obtained for control (a), LPS (b), LPS and free polyphenols, AuNPs@polyphenolsl (c), AuNPs@polyphenols and LPS (d).

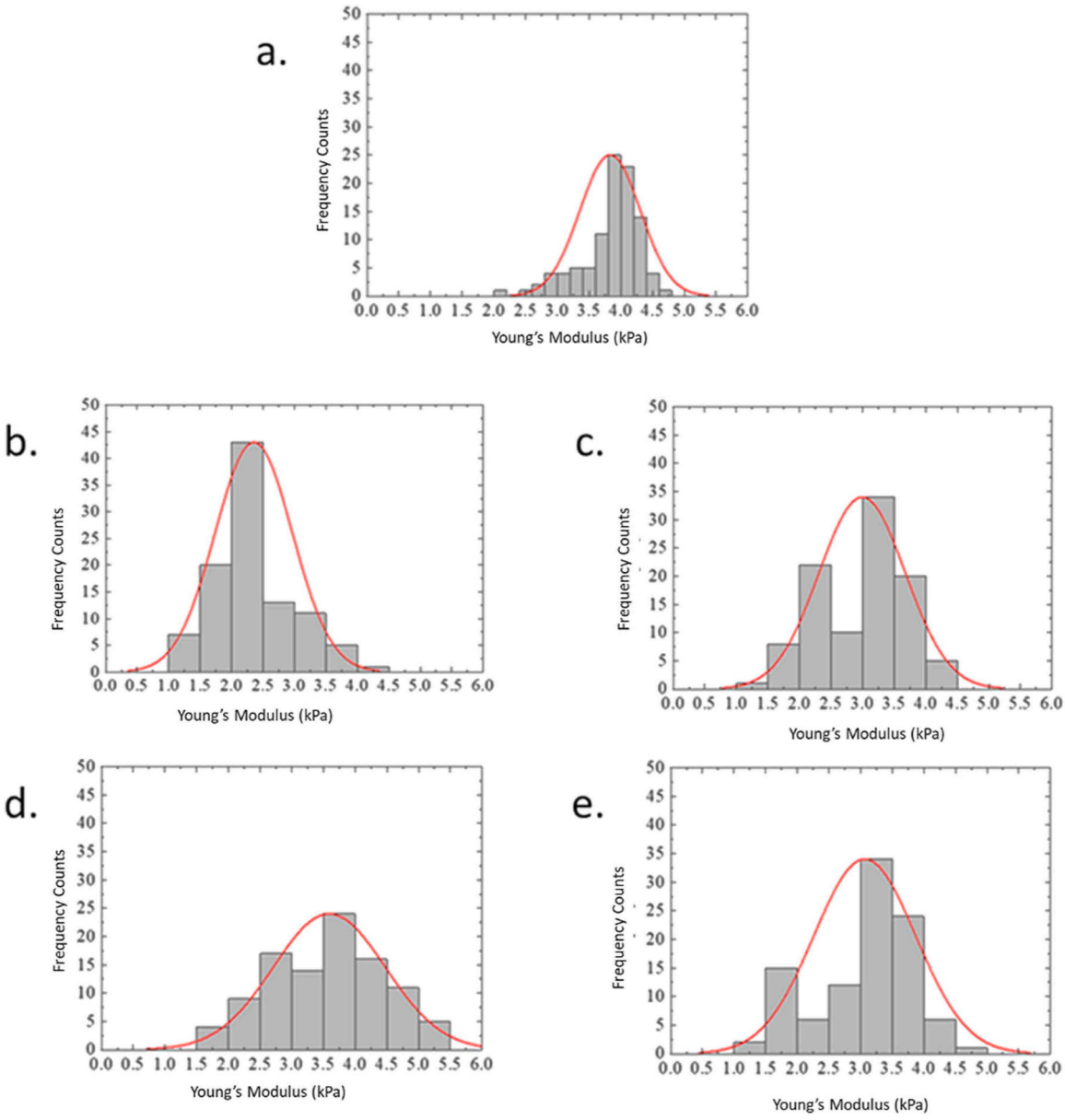

Fig. 8. Young's modulus distributions with Gaussian fit functions (blue line) for living BMDCs control (a), LPS (b), LPS and *Laurus nobilis* extract, AuNPs@polyphenols (c) and AuNPs@polyphenols and LPS (d).

Writing – review & editing, Visualization, Validation, Supervision, Software, Resources, Project administration, Funding acquisition, Formal analysis, Data curation, Conceptualization. **Mariafrancesca Cascione:** Writing – review & editing, Writing – original draft, Visualization, Validation, Software, Methodology, Formal analysis, Data curation, Conceptualization. **Valeria De Matteis:** Writing – review & editing, Writing – original draft, Visualization, Validation, Methodology, Formal analysis, Data curation, Conceptualization. **Riccardo di corato:** Validation, Methodology, Data curation, Conceptualization. **Paolo Pellegrino:** Methodology, Formal analysis, Data curation. **Massimo Catalano:** Methodology, Formal analysis, Data curation. **Aurelia Scarano:** Methodology, Formal analysis. **Alessandro Miraglia:** Methodology, Data curation.

Declaration of Competing Interest

The authors declare that they have no known competing financial interests or personal relationships that could have appeared to influence the work reported in this paper.

Data availability

Data will be made available on request.

Acknowledgment

Project PNRR-MAD-2022-12375790: "Cell specific targeting of hypoxia-induced miR-210 to modulate inflammation and fibrosis in the ischemic Heart" - PIANO NAZIONALE DI RIPRESA E RESILIENZA (PNRR), MISSIONE 6 - COMPONENTE 2 INVESTIMENTO 2.1 VALORIZZAZIONE E POTENZIAMENTO DELLA RICERCA BIOMEDICA DEL SSN; Project PNRR-MAD-2022–12376791 "Changing the future of intestinal failure in intestinal chronic inflammation: towards innovative predictive factors and therapeutic targets"

Valeria De Matteis kindly acknowledges Programma Operativo Nazionale (PON) Ricerca e Innovazione 2014–2020-Azione IV.6

"Contratti su tematiche green"-DM 1062/2021 for sponsoring her salary and work

Mariafrancesca Cascione kindly acknowledgesProject PRP@CERIC - Pathogen Readiness Platform for CERIC ERIC Upgrade" – Prot. IR0000028 - PRP@CERIC, – NextGenerationEU; Project Italian MUR - PON "Ricerca e Innovazione 2014–2020" potenziamento di infrastrutture di ricerca, Azione II.1. (2019–2021) "Bio Open Lab" - CERIC-ERIC - Central European Research Infrastructure Consortium for sponsoring her salary and work

References

[1] V.C. Thipe, A.R. Karikachery, P. Çakılkaya, U. Farooq, H.H. Genedy, N. Kaeokhamloed, D.-H. Phan, R. Rezwan, G. Tezcan, E. Roger, et al., Green nanotechnology—an innovative pathway towards biocompatible and medically relevant gold nanoparticles, J. Drug Deliv. Sci. Technol. *70* (2022) 103256, https://doi.org/10.1016/j.jddst.2022.103256.

[2] P.T. Anastas, E.S. Beach, Green chemistry: the emergence of a transformative framework, Green. Chem. Lett. Rev. *1* (2007) 9–24, https://doi.org/10.1080/17518250701882441.

[3] B.A. de Marco, B.S. Rechelo, E.G. Tótoli, A.C. Kogawa, H.R.N. Salgado, Evolution of green chemistry and its multidimensional impacts: a review, Saudi Pharm. J. *27* (2019) 1–8, https://doi.org/10.1016/j.jsps.2018.07.011.

[4] Bhardwaj B., Singh P., Kumar A., Kumar S, B.V.. Eco-Friendly Greener Synthesis of Nanoparticles. *Adv Pharm Bull.* 10, 566-576.

[5] V.P. Aswathi, S. Meera, C.G.A. Maria, M. Nidhin, Green synthesis of nanoparticles from biodegradable waste extracts and their applications: a critical review, Nanotechnol. Environ. Eng. (2022) 1–21.

[6] S. Mahmood Ansari, Q. Saquib, V. De Matteis, H. Awad Alwathnani, S. Ali Alharbi, A. Ali Al-Khedhairy, Marine macroalgae display bioreductant efficacy for fabricating metallic nanoparticles: intra/extracellular mechanism and potential biomedical applications, Bioinorg. Chem. Appl. *2021* (2021) 5985377, https://doi.org/10.1155/2021/5985377.

[7] B.M. Gel, G.S. Priya, A. Kanneganti, K.A. Kumar, K.V. Rao, S. Bykkam, Bio synthesis of cerium oxide nanoparticles using aloe, Int. J. Sci. Res. Publ. *4* (2014) 1–4.

[8] M.B. Gawande, S.N. Shelke, R. Zboril, R.S. Varma, Microwave-assisted chemistry: synthetic applications for rapid assembly of nanomaterials and organics, Acc. Chem. Res. *47* (2014) 1338–1348, https://doi.org/10.1021/ar400309b.

[9] S.F. Ahmed, M. Mofijur, N. Rafa, A.T. Chowdhury, S. Chowdhury, M. Nahrin, A.B. M.S. Islam, H.C. Ong, Green approaches in synthesising nanomaterials for environmental nanobioremediation: technological advancements, applications, benefits and challenges, Environ. Res. *204* (2022) 111967, https://doi.org/10.1016/j.envres.2021.111967.

[10] K.D. Lee, P.C. Nagajyothi, T.V.M. Sreekanth, S. Park, Eco-friendly synthesis of gold nanoparticles (AuNPs) using Inonotus obliquus and their antibacterial, antioxidant and cytotoxic activities, J. Ind. Eng. Chem. *26* (2015) 67–72, https://doi.org/10.1016/j.jiec.2014.11.016.

[11] U.M. Muddapur, S. Alshehri, M.M. Ghoneim, M.H. Mahnashi, M.A. Alshahrani, A. A. Khan, S.M.S. Iqubal, A. Bahafi, S.S. More, I.A. Shaikh, et al., Plant-based synthesis of gold nanoparticles and theranostic applications: a review, Molecules *27* (2022), https://doi.org/10.3390/molecules27041391.

[12] R. Javed, M. Zia, S. Naz, S.O. Aisida, N. ul Ain, Q. Ao, Role of capping agents in the application of nanoparticles in biomedicine and environmental remediation: recent trends and future prospects, J. Nanobiotechnology *18* (1) (2020) 15, https://doi.org/10.1186/s12951-020-00704-4.

[13] D. Wu, J. Zhou, M.N. Creyer, W. Yim, Z. Chen, P.B. Messersmith Ef, J.V. Jokerst, Phenolic-enabled nanotechnology: versatile particle engineering for biomedicine, Chem. Soc. Rev. *50* (2021) 4432–4483, https://doi.org/10.1039/d0cs00908c.

[14] Dykman, L.A.; Khlebtsov, N.G. Gold Nanoparticles in Biology and Medicine: Recent Advances and Prospects. 2011, 3, 34–55.

[15] Lin, G.; Wang, J.; Yang, Y.; Zhang, Y.; Sun, T. Advances in dendritic cell targeting nano-delivery systems for induction of immune tolerance. 2023, 1–16, doi: 10.3389/fbioe.2023.1242126.

[16] B.S. Zolnik, A. González-Fernández, N. Sadrieh, M.A. Dobrovolskaia, Nanoparticles and the immune system, Endocrinology *151* (2010) 458–465, https://doi.org/10.1210/en.2009-1082.

[17] A. Merecz-Sadowska, P. Sitarek, T. Śliwiński, R. Zajdel, Anti-Inflammatory Activity of Extracts and Pure Compounds Derived from Plants via Modulation of Signaling Pathways, Especially PI3K/AKT in Macrophages, Int. J. Mol. Sci. *21* (2020), https://doi.org/10.3390/ijms21249605.

[18] H. Shakoor, J. Feehan, V. Apostolopoulos, C. Platat, A.S. Al Dhaheri, H.I. Ali, L. C. Ismail, M. Bosevski, L. Stojanovska, Immunomodulatory Effects of Dietary Polyphenols, Nutrients *13* (2021), https://doi.org/10.3390/nu13030728.

[19] Scarano, A.; Chieppa, M. Plant Polyphenols-Biofortified Foods as a Novel Tool for the Prevention of Human Gut Diseases. 2020.

[20] M. Rudrapal, S.J. Khairnar, J. Khan, A.Bin Dukhyil, M.A. Ansari, M.N. Alomary, F. M. Alshabrmi, S. Palai, P.K. Deb, R. Devi, Dietary Polyphenols and Their Role in Oxidative Stress-Induced Human Diseases: Insights Into Protective Effects, Antioxidant Potentials and Mechanism(s) of Action, Front. Pharmacol. *13* (2022) 806470, https://doi.org/10.3389/fphar.2022.806470.

[21] P.B. Bhosale, S.E. Ha, P. Vetrivel, H.H. Kim, S.M. Kim, G.S. Kim, Functions of polyphenols and its anticancer properties in biomedical research: a narrative review, Transl. Cancer Res. *9* (2020) 7619–7631, https://doi.org/10.21037/tcr-20-2359.

[22] M.H. Cháirez-Ramírez, K.G. de la Cruz-López, A. García-Carrancá, Polyphenols as Antitumor Agents Targeting Key Players in Cancer-Driving Signaling Pathways, Front. Pharmacol. *12* (2021) 710304, https://doi.org/10.3389/fphar.2021.710304.

[23] M. D'Archivio, C. Filesi, R. Varì, B. Scazzocchio, R. Masella, Bioavailability of the polyphenols: status and controversies, Int. J. Mol. Sci. *11* (2010) 1321–1342, https://doi.org/10.3390/ijms11041321.

[24] M. Claudine, W. Gary, M. Christine, S. Augustin, R. Christian, Bioavailability and bioefficacy of polyphenols in humans. I. Review of 97 bioavailability studies 1 – 3, 230S-242S, Am. J. Clin. Nutr. *81* (2005), https://doi.org/10.1093/ajcn/81.1.230S.

[25] I. Khmelinskii, V.I. Makarov, On the Effects of Mechanical Stress of Biological Membranes in Modeling of Swelling Dynamics of Biological Systems, Sci. Rep. *10* (2020) 8395, https://doi.org/10.1038/s41598-020-65217-4.

[26] S. Burns, S.J. Hardy, J. Buddle, K.L. Yong, G.E. Jones, A.J. Thrasher, Maturation of DC is associated with changes in motile characteristics and adherence, Cell Motil. Cytoskelet. *57* (2004) 118–132, https://doi.org/10.1002/cm.10163.

[27] X. Xu, Z. Zeng, W. Yao, X. Wang, D. Sun, W. Ka, Y. Zhang, X. Wang, X. Chen, Y. Zha, et al., Biomechanical alterations of dendritic cells by co-culturing with K562 CML cells and their potential role in immune escape, J. Biomech. *43* (2010) 2339–2347, https://doi.org/10.1016/j.jbiomech.2010.04.028.

[28] M. Chakraborty, K. Chu, A. Shrestha, I. Jurisica, S. Tsai, D.A. Winer, Mechanical Stiffness Controls Dendritic Cell Metabolism and Function, CellReports *34* (2021) 108609, https://doi.org/10.1016/j.celrep.2020.108609.

[29] L.M. Magalhães, F. Santos, M.A. Segundo, S. Reis, J.L.F.C. Lima, Rapid microplate high-throughput methodology for assessment of Folin-Ciocalteu reducing capacity, Talanta *83* (2010) 441–447, https://doi.org/10.1016/j.talanta.2010.09.042.

[30] V.L. Singleton, R. Orthofer, R.M. Lamuela-Raventós, Analysis of total phenols and other oxidation substrates and antioxidants by means of folin-ciocalteu reagent, in: Oxidants and Antioxidants Part A, Vol. 299, Methods in Enzymology; Academic Press, 1999, pp. 152–178.

[31] B. Cappella, M. Kappl, Force measurements with the atomic force microscope, Tech., Interpret. Appl. *59* (2005) 1–152, https://doi.org/10.1016/j.surfrep.2005.08.003.

[32] A. Wu, L. March, X. Zheng, J. Huang, X. Wang, J. Zhao, F. M.Blyth, E. Smith, R. Buchbinder, D. Hoy, Principles and practice of greener ionic liquid–nanoparticles biosystem. Nature *388* (2020) 1–14.

[33] R. Mohammadinejad, S. Karimi, S. Iravani, R.S. Varma, Plant-derived nanostructures: types and applications, Green. Chem. *18* (2016) 20–52, https://doi.org/10.1039/C5GC01403D.

[34] J.H. Xulu, T. Ndongwe, K.M. Ezealisiji, V.J. Tembu, N.P. Mncwangi, B.A. Witika, X. Siwe-Noundou, The Use of Medicinal Plant-Derived Metallic Nanoparticles in Theranostics, Pharmaceutics *14* (2022), https://doi.org/10.3390/pharmaceutics14112437.

[35] X. Xie, J. Liao, X. Shao, Q. Li, Y. Lin, The Effect of shape on Cellular Uptake of Gold Nanoparticles in the forms of Stars, Rods, and Triangles, Sci. Rep. *7* (2017) 1–9, https://doi.org/10.1038/s41598-017-04229-z.

[36] S. Zhang, H. Gao, G. Bao, Physical Principles of Nanoparticle Cellular Endocytosis, ACS Nano *9* (2015) 8655–8671, https://doi.org/10.1021/acsnano.5b03184.

[37] F.R. Delvecchio, E. Vadrucci, E. Cavalcanti, S. De Santis, D. Kunde, M. Vacca, J. Myers, F. Allen, G. Bianco, A.Y. Huang, et al., Polyphenol administration impairs T-cell proliferation by imprinting a distinct dendritic cell maturational profile, Eur. J. Immunol. *45* (2015) 2638–2649, https://doi.org/10.1002/eji.201545679.

[38] G. Verna, M. Liso, E. Cavalcanti, G. Bianco, V. Di Sarno, A. Santino, P. Campiglia, M. Chieppa, Quercetin Administration Suppresses the Cytokine Storm in Myeloid and Plasmacytoid Dendritic Cells, Int. J. Mol. Sci. *22* (2021), https://doi.org/10.3390/ijms22158349.

[39] V. De Matteis, M. Cascione, L. Rizzello, D.E. Manno, C. Di Guglielmo, R. Rinaldi, Synergistic Effect Induced by Gold Nanoparticles with Polyphenols Shell during Thermal Therapy: Macrophage Inflammatory Response and Cancer Cell Death Assessment, Cancers (Basel) *13* (2021) 3610.

[40] S. Akira, Mammalian Toll-like receptors, Curr. Opin. Immunol. *15* (2003) 5–11, https://doi.org/10.1016/S0952-7915(02)00013-4.

[41] M.K. Kim, J. Kim, Properties of immature and mature dendritic cells: phenotype, morphology, phagocytosis, and migration, RSC Adv. *9* (2019) 11230–11238, https://doi.org/10.1039/C9RA00818G.

[42] E. Cavalcanti, E. Vadrucci, F.R. Delvecchio, F. Addabbo, S. Bettini, R. Liou, V. Monsurrò, A.Y.C. Huang, T.T. Pizarro, A. Santino, et al., Administration of reconstituted polyphenol oil bodies efficiently suppresses dendritic cell inflammatory pathways and acute intestinal inflammation, PLoS One *9* (2014), https://doi.org/10.1371/journal.pone.0088898.

[43] V. Galleggiante, S. De Santis, E. Cavalcanti, A. Scarano, M. De Benedictis, G. Serino, M.L. Caruso, M. Mastronardi, A. Pinto, P. Campiglia, et al., Dendritic Cells Modulate Iron Homeostasis and Inflammatory Abilities Following Quercetin Exposure, Curr. Pharm. Des. *23* (2017) 2139–2146, https://doi.org/10.2174/1381612823666170112125355.

[44] J.L. Rodríguez-Fernández, O. Criado-García, The Actin Cytoskeleton at the Immunological Synapse of Dendritic Cells, Front. Cell Dev. Biol. *9* (2021) 679500, https://doi.org/10.3389/fcell.2021.679500.

[45] K.L. Hui, L. Balagopalan, L.E. Samelson, A. Upadhyaya, Cytoskeletal forces during signaling activation in Jurkat T-cells, Mol. Biol. Cell *26* (2015) 685–695, https://doi.org/10.1091/mbc.E14-03-0830.

[46] D.W. O'Neill, S. Adams, N. Bhardwaj, Manipulating dendritic cell biology for the active immunotherapy of cancer, Blood *104* (2004) 2235–2246, https://doi.org/10.1182/blood-2003-12-4392.
[47] H.J. Crespo, J.T.Y. Lau, P.A. Videira, Dendritic cells: a spot on sialic Acid, Front. Immunol. *4* (2013) 491, https://doi.org/10.3389/fimmu.2013.00491.
[48] Y. Yamakita, F. Matsumura, M.W. Lipscomb, P. Chou, G. Werlen, J.K. Burkhardt, S. Yamashiro, Fascin1 promotes cell migration of mature dendritic cells, J. Immunol. *186* (2011) 2850–2859, https://doi.org/10.4049/jimmunol.1001667.
[49] M. Song, Dendritic Cell-Based Immunotherapy, Import. Dendritic Cell Migr. *2024* (2024).
[50] A. Leblanc-Hotte, C. Audiger, G. Chabot-Roy, F. Lombard-Vadnais, J.S. Delisle, Y. A. Peter, S. Lesage, Immature and mature bone marrow-derived dendritic cells exhibit distinct intracellular mechanical properties, Sci. Rep. *13* (1) (2023) 11, https://doi.org/10.1038/s41598-023-28625-w.
[51] A.Jansen Karin, M.Donato Dominique, E.Balcioglu Hayri, Schmidt Thomas, G.H. K. Erik H.J. Danen, A guide to mechanobiology: where biology and physics meet, Biochim. Biophys. Acta - Mol. Cell Res. *1853* (2015) 3043–3052.
[52] Cascione, M.; Leporatti, S.; Dituri, F.; Giannelli, G. Molecular Sciences Transforming Growth Factor-β Promotes Morphomechanical Effects Involved in Epithelial to Mesenchymal Transition in Living Hepatocellular Carcinoma., doi:10.3390/ijms20010108.
[53] De Matteis, V.; Cascione, M.; Chiara, &; Toma, C.; Leporatti, S. Morphomechanical and organelle perturbation induced by silver nanoparticle exposure., doi:10.1007/s11051-018-4383-3.
[54] A.F. Pegoraro, P. Janmey, D.A. Weitz, Mechanical properties of the cytoskeleton and cells, Cold Spring Harb. Perspect. Biol. *9* (2017), https://doi.org/10.1101/cshperspect.a022038.
[55] Cascione, M.; Matteis, V.D.E.; Rinaldi, R.; Leporatti, S. Atomic force microscopy combined with optical microscopy for cells investigation Atomic Force Microscopy Combined with Optical Microscopy for Cells Investigation. 2016, doi:10.1002/jemt.22696.
[56] G. Guan, Y. He, L. Mei, Atomic force microscopy: a nanobiotechnology for cellular, Nano TransMed *1* (2022) e9130004, https://doi.org/10.26599/NTM.2022.9130004.
[57] M. Liso, A. Sila, VerAdministration, G. a Pilot Study.na, A. Scarano, R. Donghia, F. Castellana, E. Cavalcanti, P.L. Pesole, E.M. Sommella, A. Lippolis, et al., Nutritional regimes enriched with antioxidants as an efficient adjuvant for IBD patients under infliximab, Antioxidants (Basel, Switzerland) (2022) *11*, https://doi.org/10.3390/antiox11010138.